Colloidal Gelation as a General Approach to the Production of Porous Materials

Daniel F. Schmidt,*[,†,‡] Cedric du Fresne von Hohenesche,[†,§] Axel Weiss,[||] and Volker Schädler[†,⊥]

BASF-ISIS, 8 allee Gaspard Monge, F-67083 Strasbourg, France, and BASF AG, D-67056 Ludwigshafen, Germany

Received December 21, 2007
Revised Manuscript Received February 28, 2008

We report a simple, versatile technique that gives porous bodies from arbitrary building blocks in a highly controllable fashion. Our approach relies on controlled colloidal gelation and allows for large variations in structure and composition. This technique is capable of producing mechanically robust, highly porous monoliths with significant nanoporosity via ambient drying and is amenable to the incorporation of functional/responsive colloidal species as well. The concept of colloidal gelation ("col-gel" for short) is well-known in the area of food science[1] and has been the subject of numerous theoretical and modeling efforts.[2] The ability to gel dispersions of colloidal metal oxides is well-known.[3] Our work distinguishes itself several ways.

First, we use soluble, reactive molecular species to glue otherwise stable colloids together. In contrast, metal oxide colloids undergo gel formation via pH-sensitive equilibria between molecular and colloidal species. Second, our technique covers a wider range of compositions than has previously been reported. Third, our materials survive as monoliths following ambient drying from aqueous media, demonstrating their robust nature and the simplicity and utility of this approach. The process is shown in Scheme 1.

Here we report three variations on this theme, involving fully organic systems (polymer particles and glue) and two distinct classes of hybrids (ceramic particles and polymer glue, polymer particles and ceramic glue).

The polymer "glue" used was a melamine−formaldehyde (MF) resin supplied by BASF AG and produced through the base-catalyzed reaction of melamine, formaldehyde, and methanol in a molar ratio of 1:3.6:2.0. The MF reaction produces a mixture of methylolated melamine oligomers, which react with methanol to produce methyl ether derivatives. The end result is a clear, colorless, viscous liquid. The resin-forming reaction and a representative resin component are shown in Scheme 2a. While the polycondensation chemistry of MF resins is quite complicated and not completely understood,[4,5] a common cross-linking sequence is shown in Scheme 2, parts b (hydrolysis) and c (condensation). Typical catalytic schemes involve either weak acids and their conjugate bases or strong acids, with salts showing catalytic activity as well.[5]

The ceramic "glue" used was tetramethoxysilane (TMOS). TMOS also undergoes hydrolysis (Si−O−CH_3 → Si−OH + CH_3OH) and polycondensation (2Si−OH → Si−O−Si + H_2O), with typical catalysts again being acids, bases, and/or salts.

The polymer particles were latexes prepared from 97% styrene, 1.5% acrylic acid, and 1.5% acrylamide, with particle

Scheme 1. Colloidal Gelation ("col-gel") Process

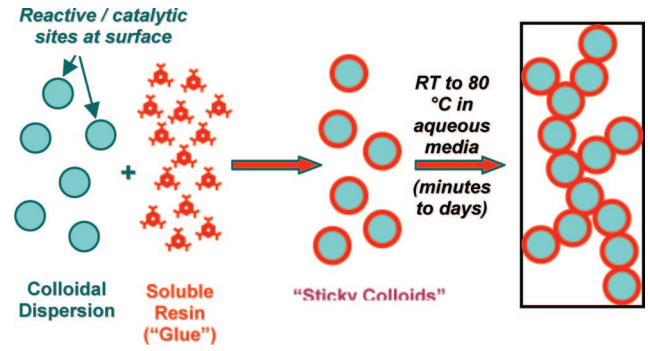

Scheme 2. Reaction Diagram for the Formation of a Monomeric Unit Representative of the Resin Used in This Work[a]

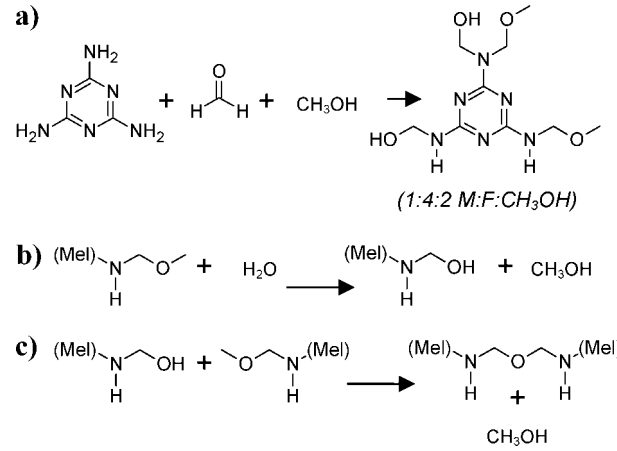

[a] Based on a melamine to formaldehyde to methanol molar ratio of 1:3.6:2.0 (a) and for the hydrolysis of a methylolmelamine methyl ether substituent (b) followed by the condensation of the resultant methylolmelamine group with a second methylolmelamine methyl ether group (c).

[†] BASF-ISIS.
[‡] Present address: Department of Plastics Engineering, University of Massachusetts Lowell, 1 University Avenue, Lowell, Massachusetts 01854.
[§] Present address: BASF Nederland B.V., Innovatielaan 1, NL-8466 SN Nijehaske, The Netherlands.
[||] BASF AG.
[⊥] Present address: BASF Corporation, 1609 Biddle Avenue, Wyandotte, Michigan 48192.

(1) Donald, A. N. *Rep. Prog. Phys.* **1994**, *57*, 1081–1135.
(2) See, for example, (a) Haw, M. D.; Sievwright, M.; Poon, W. C. K.; Pusey, P. N. *Adv. Colloid Interface Sci.* **1995**, *62*, 1–16. (b) Bergenholtz, J.; Fuchs, M. *J. Phys.: Condens. Matter* **1999**, *11*, 10171–10182. (c) Dickinson, E. *J. Colloid Interface Sci.* **2000**, *225*, 2–15. (d) Kolb, M. *Adv. Solid State Phys.* **2001**, *41*, 381–389. (e) Cates, M. E.; Fuchs, M.; Kroy, K.; Poon, W. C. K.; Puertas, A. M. *J. Phys.: Condens. Matter* **2004**, *16*, S4861–S4875.
(3) Brinker, C. J.; Scherer, G. W. *Sol-Gel Science*; Academic Press: San Diego, 1990; pp 235−301.
(4) (a) Blank, W. J.; Hensley, W. L. *J. Paint Technol.* **1974**, *46*, 46–50. (b) Blank, W. J. *J. Coat. Technol.* **1979**, *51*, 61–70.
(5) (a) Holmberg, K. In *Organic Coatings, Science and Technoly*; Parfitt, G. D., Patsis, A. V., Eds.; Marcel Dekker: New York, 1986; Vol. 8, pp 125−138. (b) Gatechair, L. R. *Proc. Int. Waterborne, High-Solids, Powder Coat. Symp.* **1988**, *15*, 33–54.

10.1021/cm7036603 CCC: $40.75
Published on Web 04/05/2008

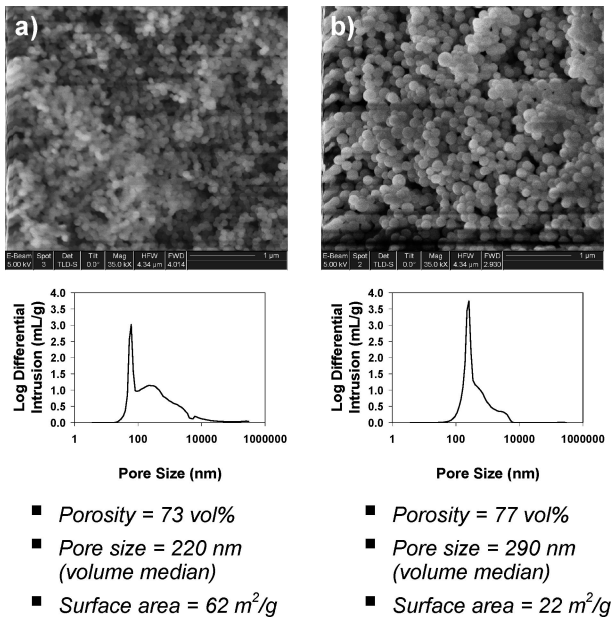

Figure 1. Representative (8000×) SEM images and mercury intrusion data from porous monoliths produced via the colloidal gelation of 120 nm polystyrene latex particles (a) and 100 nm colloidal silica particles (b) with MF resin (both from 5 vol % particles + 5 wt % resin in water).

sizes of 120, 220, and 320 nm, respectively (provided by BASF AG). The presence of carboxylic acid and amide groups and surface charges give multiple opportunities for resin polycondensation at the particle surface.

The ceramic particles were commercial aqueous silica colloids (Levasil 50S2, from H.C. Stark) with a particle size of 100 nm, treated with glycidoxypropyltrimethoxysilane to enhance their surface reactivity versus the MF resin.

In all cases, colloidal dispersions (pH ~4) and resins were diluted with deionized water (Millipore Elix, 18.2 MΩ·cm), combined and sealed in disposable plastic vials, and shaken until homogeneous. Mixtures contained 5 vol % of colloidal particles plus 5 wt % resin, with additional variations in the particle to resin ratio giving structural control. Gelation took place at room or elevated temperature (60 or 80 °C via immersion in a constant temperature water bath). Gel times ranged from less than an hour to several days, with more rapid gelation seen at higher temperatures. Once syneresis was complete (as indicated by no change in sample size over several days) the vials were opened, and the samples dried under a fume hood and then placed in a vacuum oven at 50 °C until a pressure of less than 20 torr was reached.

Rigid, colorless monoliths were produced in all cases, with porosity barely visible in systems with the largest pores (several micrometers). Some shrinkage was observed following drying, and the monoliths were easily handled and could be sectioned with a razor blade. Samples were analyzed via scanning electron microscopy (FEI Dual Beam 235 SEM, using low voltage imaging of uncoated samples), mercury intrusion porosimetry (Micromeritics Autopore IV), and nitrogen sorption (Quantachrome Autosorb-6B).

Figure 1 demonstrates the ability of the technique to produce nearly identical structures based on very different compositions. The shape of the pore size distributions shown here is typical of these materials, with the sharp peak

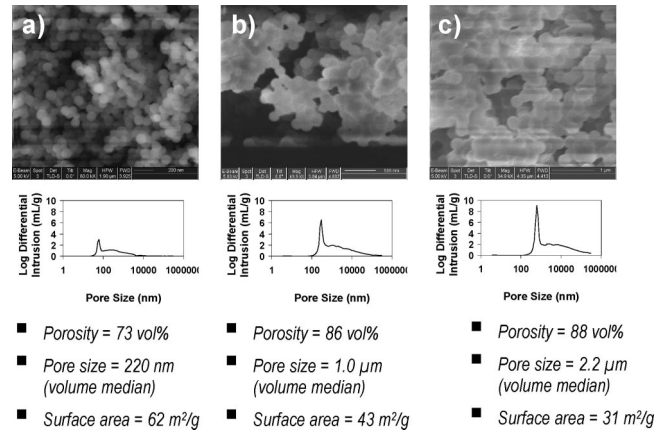

Figure 2. Representative SEM images and mercury intrusion data from porous monoliths produced via the colloidal gelation of 5 vol % 120 nm (80 000×) (a), 220 nm (50 000×) (b), and 320 nm (35 000×) (c) polystyrene latex particles with 5 wt % MF resin (1:1 mass ratio).

representing interstitial pores between primary particles and the broad shoulder representing interstitial pores between the occasional multiparticle assembly. These assignments are generally consistent with what is observed in SEM. Polystyrene latex particles appear smaller than colloidal silica due to the fact that the latex particle size indicated represents the hydrodynamic radius (via light-scattering) rather than a hard-sphere radius (clearly smaller as seen via SEM). This alone is sufficient to explain the slight reduction in porosity (due to increased drying shrinkage) and pore size and increased specific surface area in the MF−latex system vs the MF−silica system. TMOS-latex systems were also prepared successfully but were difficult to compare to MF-based systems due to differences in resin conversion and solids density. Nevertheless, SEM analysis of these systems also shows discrete particles adhered to one another rather than particles embedded in a matrix.

A second strength of this technique is the ability to induce structural alterations independent of component composition by altering the particle size or the ratio of particle to resin. This is demonstrated in Figure 2, where SEM results from a series of monoliths based on MF resin (5 wt %) in combination with 120, 220, or 320 nm polystyrene latex particles (5 vol %) are shown. As the particle size increases, the same amount of adhesive is spread over less surface area and clumping is favored. The average coordination number of a particle in the network increases as a result, giving rise to larger pores. Magnifications were chosen to emphasize this trend by making the particles appear the same size.

Figure 3 offers a more complete description of the structural variations achievable in this system. These plots were prepared using data from 29 different samples based on 19 distinct compositions (shown as black diamonds) using Origin (OriginLab, Version 7.5), a scientific plotting and analysis package, via a random *XYZ* matrix conversion/correlation gridding technique (22 × 22 grid, search radius = 2, smoothness = 1; parameters chosen to ensure close contact between data points and surface). This conversion is appropriate for data points spaced irregularly, while the correlation gridding technique is based on the Kriging

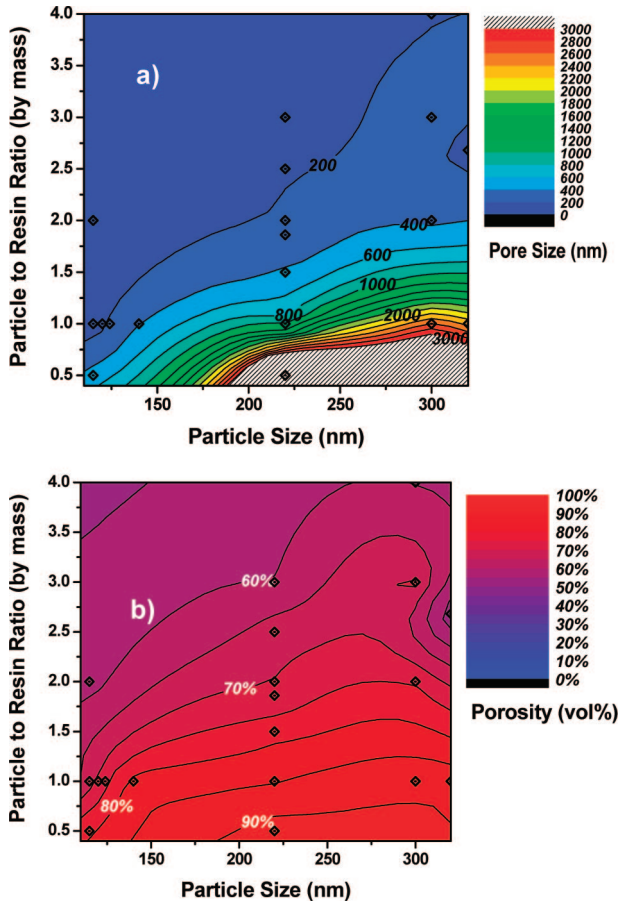

Figure 3. Topographic plots show the variation of pore size (a) and porosity (b) with particle size and particle to resin ratio for a range of polystyrene latex/MF resin systems. Data points are shown as diamonds, with data included from additional analogous polystyrene latex dispersions as well as those mentioned in the text.

method[6] for interpolating unknown Z data at given XY coordinates. The Z values of multiple data points with the same XY coordinates (i.e., replicates of a single composition) were averaged for this analysis, with reproducibility demonstrated by the data given in Table 1.

These results confirm previous arguments and again show larger pores and higher porosity (thanks to decreased drying shrinkage) with increased particle size and decreased particle to resin ratio. Given a total solids content of 10 wt % in the MF−latex systems reported here, a maximum of just over 90 vol % porosity is expected (given $\rho_{MF} \sim 1.5$ g/cm^3 and $\rho_{latex} \sim 1.0$ g/cm^3). While the data show that these levels of porosity are only achieved in samples with larger pore sizes, substantial porosity is retained across a wide range of pore sizes from less than 200 nm up to several micrometers.

(6) Davis, J. C. *Statistics and Data Analysis in Geology*, 2nd ed.; John Wiley & SonsNew York, 1986; p 383.

Table 1. Statistical Analysis of the Pore Size and Porosity of Multiple Replicates of Selected Polystyrene Latex/MF Formulations Prepared Weeks to Months Apart[a]

particle to resin ratio (by mass)	particle size (nm)	number of replicates (n)	pore size (nm)	porosity (vol %)
1	120	4	170 ± 20	71.8 ± 1.3
1	220	4	870 ± 150	84.4 ± 0.9
1	320	3	2370 ± 140	88.1 ± 0.4

[a] Errors given are standard deviations.

In sum, we present a flexible technique for the preparation of porous solids involving controlled colloidal gelation, or "col-gel" chemistry, displaying the distinct advantage of independent control over composition and structure. While further work is needed to confirm the nature of the particle/resin interactions, these results are consistent with surface-enhanced polymerization. Likewise, the lack of gelation observed when cationic latex/MF systems were combined emphasizes the importance of surface chemistry. This represents a new means of accessing the intermediate pore sizes between those of microporous zeolites and aerogels (~1–10 nm pores) and polymer foams (~10–100 μm pores).

Such materials have potential utility in a variety of applications, from filtration and separation to sorption or even thermal or acoustic insulation. Likewise, their robust nature and simple preparation procedures give them substantial advantages over both polymer foams (which cannot give such combinations of fine pores and high porosity, especially not 100% open-cell, as these are) and aerogels (which are 100% open-cell and can be produced with similar structures but require expensive and involved drying procedures and must be passivated to remain stable). This technique may therefore hold substantial promise in the future, both from a scientific standpoint and as a means of generating new and interesting porous materials otherwise difficult or impossible to produce by traditional methods.

Acknowledgment. This work was financially supported by BASF AG. We also wish to thank the Institut de Science et d'Ingénierie Supramoléculaires at the Université Louis Pasteur (Strasbourg, France) for hosting and offering support to the BASF-ISIS team during the course of this work.

CM7036603